AN EPR ORIGINAL APPROACH FOR CHARACTERIZATION OF POROUS MATERIALS AND APPLICATION TO COTTON FIBERS

N. Abidi
C. Universitaire Triolet
Montpellier France.
E. Hequet and C. Kaewprasit
Laboratory of cotton technology, CIRAD-CA,
Montpellier, France.
B. Deroide and J-V. Zanchetta
LPMC, University of Montpellier II,
Montpellier, France.

Abstract

The electron paramagnetic resonance (EPR) of Mn^{2+} was used to determine pore size distribution of silica gel and aerosil200. The paramagnetic probe Mn^{2+} was chosen because it is sensitive to its environment. In presence of water molecules, $[Mn(H_2O)_6]^{2+}$ paramagnetic species can be formed. Consequently, all of the changes of water pressure lead to modify the EPR spectra of Mn^{2+}. Using Kelvin law, a pore radius distribution can be established. By this EPR technique, the pores radius values of silica gel and aerosil200 are 5Å and 16Å respectively. The comparison between the results obtained from the EPR and BET techniques is satisfactory and seems promising. EPR technique was tried to apply to cotton fibers.

Introduction

Porosity is defined as the fraction ϵ ($\epsilon=V_p/V$) of the total volume of the sample which is attributed to the pores detected by the method used. This fraction value depends on the method used to determine the apparent volume V and on that used to access to pore volume V_p. The pore size is the distance between two opposite walls of the pore. The classification of pore sizes, based on the average width of the pores, by IUPAC (Sing et. al., 1958) is macropores which is beggar than 500Å, mesopores which is between 500 and 20Å and micropores which is less than 20Å (supermicropores >7Å, ultramicropores <7Å). Usually the pores in a material do not have the same size but exist as a distribution of size which can be wide or sharp. Pore size distribution is classically represented by the derivatives dS_p/dr_p or dV_p/dr_p as function of r_p (pores radius) where S_p and V_p are respectively the wall area and volume of the pores. The size in question is here the radius, which implies that the pores are known to be, or assumed to be, cylindrical. In other cases, r_p should be replaced by the width. Several techniques have been used to characterize porous materials (determination of porous volume, specific surface area and pore size distribution) (Lowell et. al., 1994 ; Gregg et. al., 1982). The gaz adsorption/desorption isotherm (physisorption) is one of the most important and extensively used method. Moreover, Nuclear Magnetic Resonance (NMR), which is sensitive to short range order, has been recently used to obtain information on the structure of the pores. Two main techniques of NMR can be found in the literature: one is based on the study of NMR relaxation times of a fluid inside pores (usually water) (Gallego et. al.,1988) and the other on the chemical shift of ^{129}Xe adsorbed in a material (Terskikh et. al., 1993).

Recently, we have shown that it is possible to use EPR of Mn^{2+} probe to characterize the structure of some porous materials such as silica gel and aerosil (Abidi et. al., 1997). The purpose of this work is to propose an EPR method for determination of pore size distribution and an application to cotton fiber will be reported also.

EPR Theory

EPR spectroscopy is a method of structure determination by measuring species containing unpaired electrons. It has been widely used for investigation for the structure of glasses (Griscom 1980). Since EPR spectra are sensitive to the interaction of paramagnetic probe with its environment, they can provide useful information on the changes that take place when the probe environment change. The Mn^{2+} probe are most frequently used as a probe ions because their EPR spectrum can easily be detected even at room temperature. A typical EPR spectrum of Mn^{2+}, in silica gel, is shown in ***figure 1***. The EPR spectra are recorded using a spectrometer Bruker at a frequency around 9.8 GHz (X-band). The resonant lines are obtained in a double cavity. This dual cavity allows to use of a standard for the determination of g-values ($g=h\nu/\beta H$, where h is the Planck constant, ν is the operating frequency, β is the Bohr magneton and H is the magnetic field). DPPH (α,α-diphenyl,β-picryl-hydrazyl, with a splitting factor g of 2.0036) was used as a standard for g measurements. The number of spins was determined by comparison with the signal of a secondary standard, Lapis lazuli, ($Na_8[Al_6Si_6O_{24}]S_2$) chosen for its single Lorentzian linewidth comparable to those of the studied sample.

The interpretation of such spectra (***figure 1***) is based on the spin Hamiltonian of the general form (Ferreira et. al., 1988) :

$$H = \beta\, \mathbf{H}\mathbf{g}\, S + I.\mathbf{A}.S \qquad (1)$$

where **g** is the isotropic g factor, β the Bohr magneton, H the external applied magnetic field, S and I are respectively electronic and nuclear momentum vectors, A is the hyperfine coupling tensor. The first term concerns the isotropic interaction between the electronic spin and the magnetic field, the second term concerns the coupling between the electronic and the nuclear spins. From the equation (1) and by using the perturbation theory (Rao et. al., 1987), the positions H_m of the different absorption lines can be calculated by the following equation :

Reprinted from the *Proceedings of the Beltwide Cotton Conference*
Volume 2:1594-1598 (1998)
National Cotton Council, Memphis TN

$$H_m = H_0 - A.m - \left[I(I+1) - m^2\right] \times \frac{A^2}{2H_0} \qquad (2)$$

where H_0 is the central value of the spectra so that $H_0 = h\nu/g\beta$ (g the isotropic value of the manganese ion) and m is the quantum number of the projection of S on the external magnetic field direction (for Mn^{2+} I=5/2, S=5/2 and m=±5/2, ±3/2, ±1/2). The relation (2) is used for the numerical simulation of all experimental spectra. This simulation gives the type of the responsible sites of the experimental EPR spectra. An example of calculated spectra is shown in figure 1.

Materials

Three materials were studied in this work :

1- The silica gel prepared from $Si(OC_2H_5)_4$ by sol-gel process (Abidi et. al., 1996). In this case, Mn^{2+} probe is introduced during the sol preparation in the form of $Mn(C_5H_7O_7)_2$.

2- The industrial pyrogenic silica glass (aerosil200, purchased from DEGUSSA). Mn^{2+} was introduced by impregnation. The impregnation was performed by stirring the mixture of aerosil200 and $MnCl_2$ aqueous solution, at room temperature. The impregnated glass was recovered by filtration and then air dried. Nitrogen adsorption-desorption isotherm shows a mesoporous character and a BET specific surface area of 200 m^2g^{-1}.

3- The ICCS (International Calibration Cotton Standard) named C-36. The cotton sample is extracted by ethyl ether during 8 hours, then air dried. After that, it is washed by hot water, three times, pressed and air dried again. Mn^{2+} was introduced by impregnation which is done by stirring the mixture of cotton fibers and $MnCl_2$ aqueous solution, at room temperature.

Results and Discussion

The EPR spectra of Mn^{2+} probe in silica gel is shown in ***figure 1***. The characteristic sextuplet of Mn^{2+} named hyperfine structure (hfs) arises from the interaction between the electronic and nuclear spin. The sites responsible for this absorption (sextuplet band) are noted Γ. In a previous study (Abidi et. al., 1996) the Γ sites have been ascribed to hydrated Mn^{2+} species ($[Mn(H_2O)_6]^{2+}$) in interaction with the surface of the gel. In addition, the simulation of all experimental spectra showed that it was necessary to superimpose on the hyperfine structure, a broader line characterized by g=2.00 and the linewidth equal to 500 Gauss. The sites noted Σ responsible for this broader absorption band are ascribed to Mn^{2+} species subject to spin-spin interactions (Abidi et. al., 1996).

Since the Γ sites (hfs lines) are ascribed to $[Mn(H_2O)_6]^{2+}$, they are sensitive to water vapor pressure. Consequently, the dehydration of the sample leads to the disappearance of hfs lines and the conversion Γ→Σ is taken place. However, the adsorption of water again (in this case, the sample after dehydration are put in contact with a saturated water vapor pressure at room temperature) allow the appearance of Γ sites. ***Figure 2*** shows this dehydration-hydration process for silica gel, before dehydration (***fig.2-a***), immediately after dehydration (***fig.2-b***) and as a function of the hydration time (***fig.2-c*** to ***2-e***). Similar results have been observed on the aerosil200 also.

We suppose that the conversion Γ→Σ is related to the surface dehydration of the solid, the Laplace equation (Brinker et. al., 1990) indicates that during the drying of the pores, the pressure is a reciprocal function of the pore radius. Therefore, it seems necessary to verify the validity of the envisaged assumption by following the evolution of the EPR spectra during the dehydration of the silica gel. Before EPR measurements, the samples were dried and submitted to a pressure saturated of water vapor for long time enough to obtain a well defined hyperfine structure. The pressure (P) was then decreased step by step, and the EPR spectra were recorded for each step. The total number of paramagnetic species, N, was determined for each pressure. Simulation of the spectra gave the number N_Γ of Γ sites ($N_\Gamma = \alpha N$, where α represents the percentage of Γ sites determined by simulation). ***Figure 3*** shows the variation of N_Γ when the pressure P is decreased from atmospheric pressure to the limiting value, 0.1Pa. When $P > P_0$, (P_0 is the saturated water pressure), there is no modification of the spectra. This observation seems to indicate that the probe does not diffuse in the free water region and remains located on, or near, the surface where Van der Waals interactions are more effective. Significant modifications are observed when P is lower than P_0. In this pressure domain, it seems acceptable to suppose that drying leads to the draining of the probe (from Γ sites) towards the pores which are not yet empty (Σ sites). The disappearance of the hyperfine structure (***fig. 2-b***) was well explained by this phenomenon. If this hypothesis is correct, we get more precise information on the pore radius distribution. N_Γ decreases during the dehydration (i.e. when the outgassing pressure is decreased). The draining of the pores containing the probe is gouverned by Kelvin's law. So it is possible to correlate the number of water free pores of a given radius to the water vapor pressure on the sample.

In general, a pore radius can be calculated by the Kelvin equation (Brinker et. al., 1990) :

$$\ln \frac{P}{p_0} = -\frac{\beta \gamma_{LV} V_m}{rRT} \qquad (3)$$

where P is the pressure for which the vaporization occurs, β is the geometrical factor depending on the shape of the meniscus formed by the liquid in the capillary (β=1 for slit-shaped pores, β=2 for cylindrical pores), γ_{LV} is the surface tension of the condensed liquid at the absolute temperature

T, V_m is the molar volume of condensed liquid at T (water in our case), r is the Kelvin radius (dimension characteristic of the capillary) and R the ideal gas constant.

Or,
$$r = -\frac{2\gamma_{LV} V_m}{RT \ln \frac{P}{p_0}} \qquad (4)$$

In order to establish the distribution of the pore radius, the variation of the number of paramagnetic sites Γ can be written as follow:

$$\frac{dN_\Gamma}{dr} = \frac{dN_\Gamma}{dP} \times \frac{dP}{dr} \qquad (5)$$

By using expressions (3) and (4) we can find:

$$\frac{dN_\Gamma}{dr} = -\left[\frac{P}{r} \ln \frac{P}{p_0}\right] \frac{dN_\Gamma}{dP} \qquad (6)$$

The curve $N_\Gamma = f(P)$ of figure 3 was represented by polynomial function, and the derivative dN_Γ/dP calculated. The curve dN_Γ/dr against r, which is given by equation (6) represents the pore radius distribution. For silica gel, this curve is shwon in ***figure 4*** and indicates an average pore radius of 5Å. This value indicates a microporous character of silica gel. The corresponding result obtained by BET measurements is also indicated in the figure 4 and shows an average pore radius around 10Å. This discreppancy can be explain by the fact that BET equation is mainly applicable for mesoporous and macroporous materials.

The same experiments were performed on a aerosil200 having large pores. This glass was doped with Mn^{2+} by impregnation and submitted to the same hydration-dehydration cycles. The pore radius distribution obtained from this sample is shown in ***figure 5***. The average pore radius is estimated to 16Å and this result indicates a wider distribution of pore radius and confirms the mesoporous character of aerosil200. Comparison with the results obtained from BET measurements shows a qualitative good agreement with the results obtained from the EPR measurements. As EPR technique can indicate well the porous character of solid, we will apply this technique to determine pore radius distribution of cotton fibers.

The cotton fibers is considered like porous materials with a large capillary surface area. Many techniques were used to measure the pore size such as liquid chromatography (Ladish et. al., 1992), X-rays diffraction (Zahn 1988), gas adsorption/desorption (Merchant 1957) etc. The pore radius determined by these techniques is in the range 12Å-25Å. But there are difficulties and inconveniences of each methods. Thus, EPR technique was tried to apply.

The same experiments as described previously were performed on C-36 cotton fibers which have specific surface area of 32.42 m²/g determined by methylene bleu adsorption (Kaewprasit 1997). The EPR spectra of Mn^{2+} adsorbed in cotton fibers and of showing the dehydration-hydration process are presented in ***figure 6***. The variation of the number of Γ sites whith the dehydration pressure is gave in ***figure 7***. The pores radius distribution obtained from EPR is shwon in ***figure 8***. This curve indicates an average pore radius egal to 8Å which indicates a microporous character of C-36 cotton fibers.

Conclusion

The EPR investigation of H_2O adsorption/desorption on porous materials allows to elaborate a pore radius distribution method. This method is based on Kelvin's law and the comparison between the EPR and BET measurements seems to be promising. Of course, this is a first attempt to determine the pore radius distribution by this technique and we continue our reasearch for other types of porous materials.

References

Abidi, N., B. Deroide, J.V. Zanchetta. 1997. The interaction of Mn^{2+} with porous silica xerogels and the hydration-dehydration process in the xerogels. J. Non-Cryst. Solids. 221:59-69.

Abidi, N., B. Deroide, J.V. Zanchetta, D. Bourret, H. Elmkami, and P. Rumori. 1996. EPR study of Mn^{2+} doped silica glasses prepared by the sol-gel process. Phys. Chem. Glasses. 37(4): 149-54.

Brinker, C.G., G.W. Sherer. 1990. Sol-gel Science, the Physics and Chemistry of sol-gel Processing. Academic Press, N.Y.

Ferreira Da silva, M.G., and J.M.F. Navaro. 1988. J. Non-Cryst.Solids. 100: 447-52.

Gallegos, D.P., D.M. Smith and C.J. Brinker. 1988. A NMR technique for the analysis of pore structure : application to mesopores and micropres. J. Colloid Interface Sci. 124(1): 186.

Gregg, S.J. and K.S.W. Sing. 1982. Adsorption, Surface Area and Porosity. Academic Press, London.

Griscom, D.L., 1980. Electron Spin Resonance in glasses. J. Non-Cryst. Solids. (31):241.

Kaewprasit, C. 1997. The contribution of cotton fiber specific surface area estimation ; relation between surface area and physical properties. Ph. D. thesis. Montpellier. France. 182 pp.

Ladish, C.M, Y. Yang, A. Velayudhan and M.R. Ladish. 1992. A New Approach to the study of Textile Properties with Liquid Chromatography, Textile Research. 62(6):361-369.

Lowell, S. and J.E. Shieds. 1994. Powder Surface Area and Porosity. 2nd edn. Powder Technology Series. Chapman & Hall. London.

Merchant, M.V. 1957. A study of water swollen cellulose fibers which have been liquid-exchanged and dried from hydrocarbons. TAPPI. 40:771-781.

Rao, J.L., B. Sreedahar, Y.C. Ratnakar and S.V.J. Lakshman. 1987. J. Non-Cryst. Solids. 92: 175-9.

Sing, K.S.W., D.H. Everett, R.A.W. Hand, L. Moscow, R.A. Pierotti, J. Rouquerol and T. Sienieniewska. 1958. Reporting physisorption data for gaz/liquid systems with special reference to the determination of surface and porosity. Pure Appl. Chem. 57: 603.

Terskikh, V.V., I.L. Mudrakovskii and V.M. Mastikhin. 1993. ^{129}Xe NMR Magnetic Resonance studies of the porous structure of silica gels. J. Chem. Soc. Faraday Trans. 89(23): 4239.

Zhan, H., 1988. Lastest findings on the micro-structure of cotton. International cotton conference, Bremen. p. 1-12

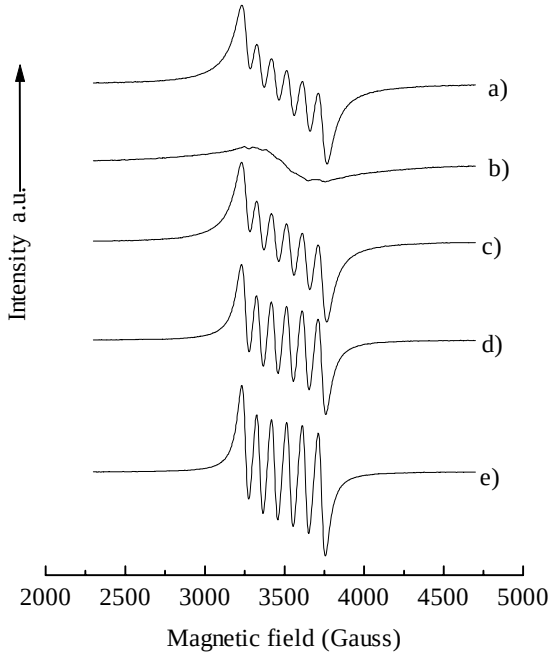

Figure 2. EPR spectra of Mn^{2+} in silica gel. a) before dehydration, b) after dehydration (P=0.1Pa), c) hydration time t=170h, d) t=375h, e) t=500h.

.

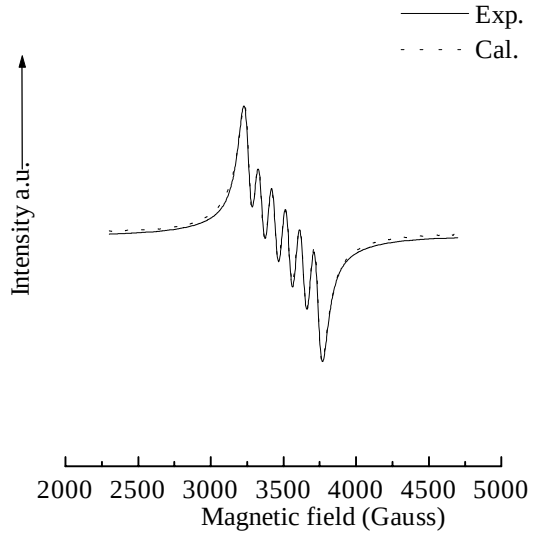

Figure 1 . EPR spectra of Mn^{2+} in silica gel at room temperature.

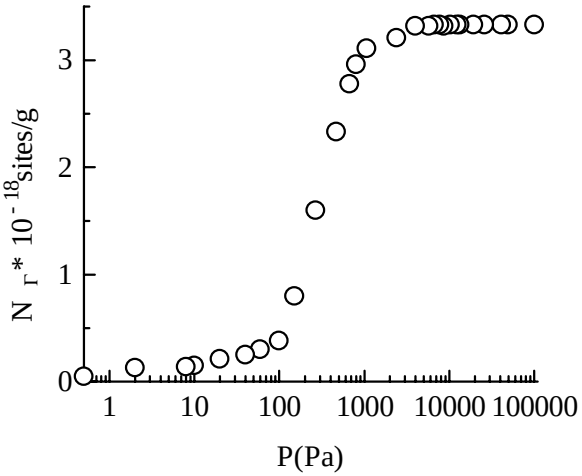

Figure 3 .Variation of the number N_Γ of Γ sites with the pressure.

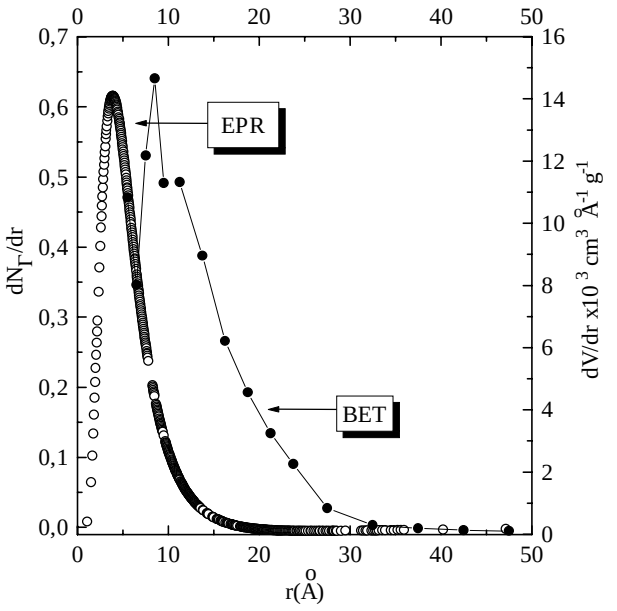

Figure 4 . Pore radius distribution obtained on silica gel from EPR and BET measurments.

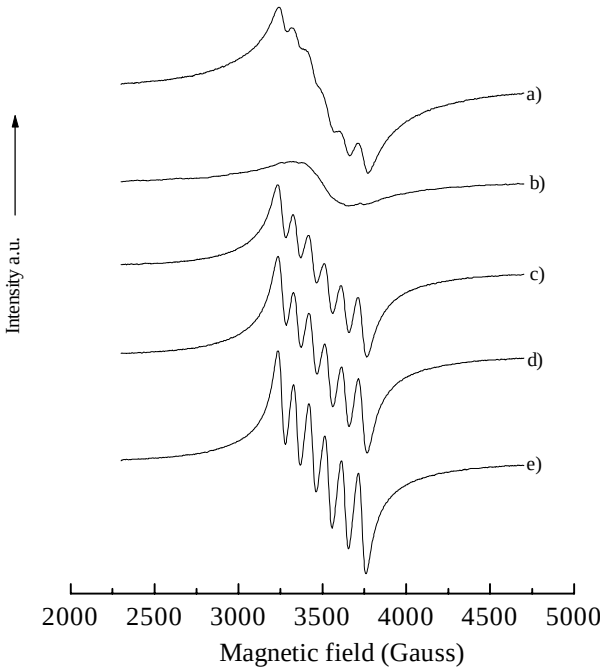

Figure 6 . EPR spectra of Mn^{2+} in C-36 cotton fibers. a) before dehydration, b) after dehydration (P=0.1Pa), c) hydration time t=310h, d) t=446h, e) t=762h.

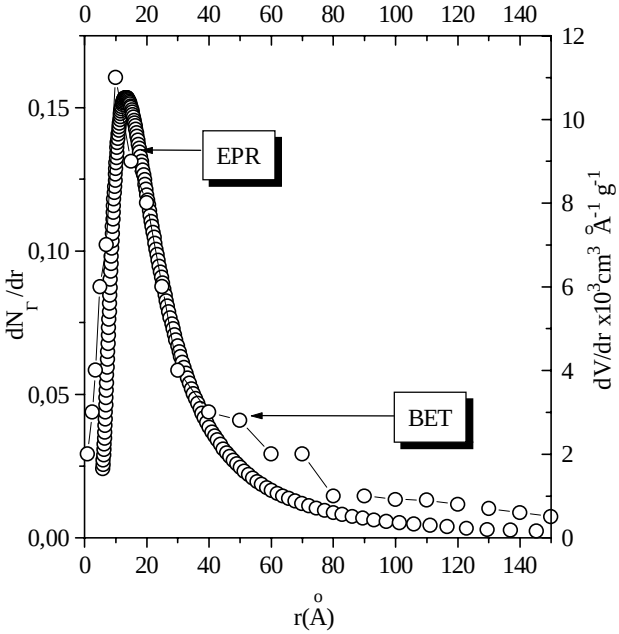

Figure 5 . Pore radius distribution obtained on aerosil200 from EPR and BET measurments.

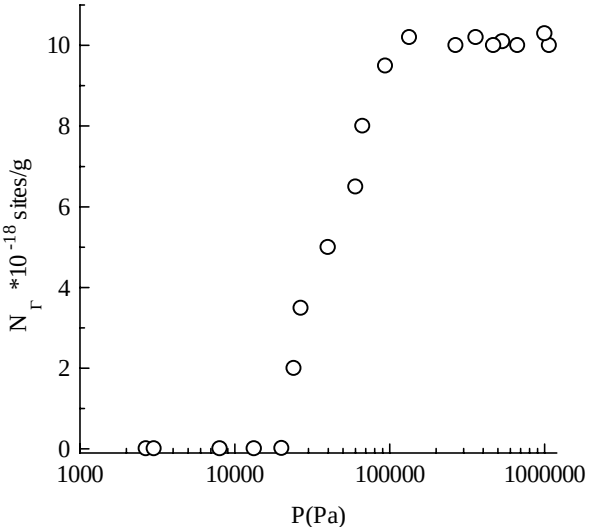

Figure 7 .Variation of the number N_Γ of Γ sites with the pressure.

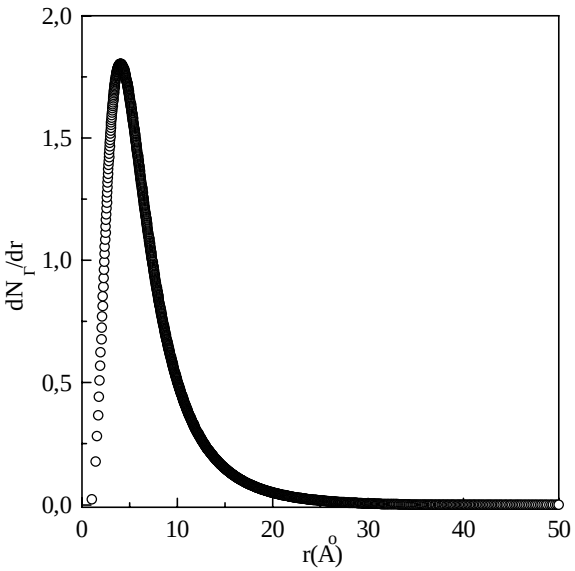

Figure 8 . Pore radius distribution obtained on C-36 cotton fibers from EPR.